Spectrochimica Acta Part A: Molecular and Biomolecular Spectroscopy 268 (2022) 120695

Contents lists available at ScienceDirect

Spectrochimica Acta Part A: Molecular and Biomolecular Spectroscopy

journal homepage: www.elsevier.com/locate/saa

Forensic examination of textile fibres using Raman imaging and multivariate analysis

Félix Zapata [a,*], Fernando E. Ortega-Ojeda [b,c,d], Carmen García-Ruiz [c,d]

[a] Department of Analytical Chemistry, University of Murcia, 30100 Murcia, Spain
[b] University of Alcalá, Department of Physics and Mathematics, Ctra. Madrid-Barcelona km 33.6, 28871 Alcalá de Henares (Madrid), Spain
[c] University of Alcalá, University Institute of Research in Police Sciences (IUICP), Ctra. Madrid-Barcelona km 33.6, 28871 Alcalá de Henares (Madrid), Spain
[d] University of Alcalá, Department of Analytical Chemistry, Physical Chemistry and Chemical Engineering, Ctra. Madrid-Barcelona km 33.6, 28871 Alcalá de Henares (Madrid), Spain

HIGHLIGHTS

- Raman Imaging combined with multivariate analysis has been proven as a promising tool for discriminating textile fibres and fabrics.
- The discrimination of fibres by Raman is assisted by both the clothing material and their dyes.
- Fibres of the same material composition but different colour are distinguished.
- Fibres of the same perceptible colour but different material composition are also distinguished.
- Raman imaging has enabled the chemical visualization of a particular fibre in contrast to others.

GRAPHICAL ABSTRACT

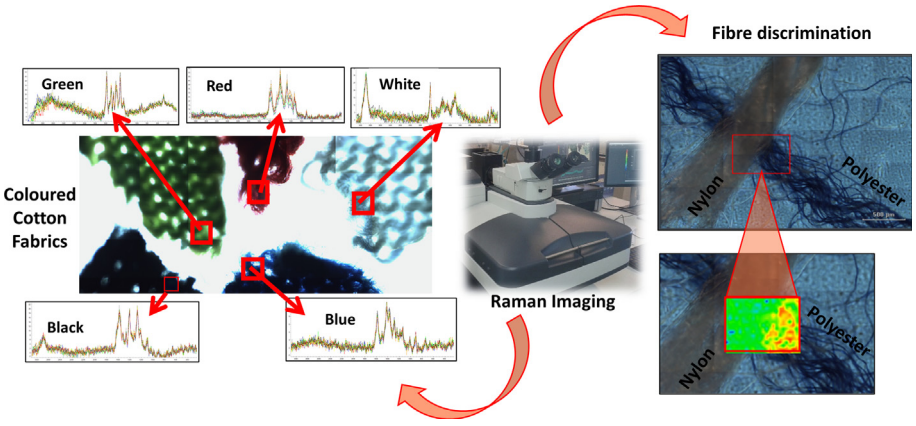

ARTICLE INFO

Article history:
Received 24 August 2021
Received in revised form 26 November 2021
Accepted 30 November 2021
Available online 03 December 2021

Keywords:
Raman imaging
Chemometrics
PCA
MCR
MANOVA
Cotton
Nylon
Polyester
Silk
Acrylic

ABSTRACT

Vibrational spectroscopic techniques have shown to be highly suitable for the identification and comparison of textile fibres and clothing fabrics. On the other hand, new chemical imaging modes based on these spectroscopic techniques are becoming useful in multiple fields. This is particularly important to, for instance, chemically visualize and screen different samples including forensic evidence (crime scene investigation), chemical and food products (quality control), biological tissues and living beings (medical imaging), among others. This study explores the forensic examination and selective chemical visualization of textile fibres and clothing fabrics using Raman imaging. Four experiments were performed, which were focused on the screening of (i) white different materials made of 100 % cotton (gauze, cotton wool, t-shirt, and swab), (ii) polyester and cotton fabrics evidence of the same colour, (iii) five different coloured cotton fabrics, and (iv) textile fibres of different materials (acrylic, cotton, nylon, polyester, and silk). Several methods of multivariate chemometric analysis including principal component analysis (PCA), multivariate analysis of variance (MANOVA), and multivariate curve resolution (MCR) were applied to enhance the limited visual comparison of the spectra accomplished with the unaided eye. The results evidenced the suitability of Raman imaging to statistically discriminate textile fibres and fabrics due to the chemical composition of both the clothing material and the dyestuff.

* Corresponding author.
E-mail address: felix.zapata@um.es (F. Zapata).
URL: https://cinquifor.uah.es (F. Zapata).

https://doi.org/10.1016/j.saa.2021.120695
1386-1425/

1. Introduction

Textile fibres are usual evidence in crime scene investigations, which usually provide useful information to recreate the crime events since their presence may prove the contact between people and a crime scene [1–8]. Particularly, textile fibres are highly relevant in crimes such as kidnapping, rape and homicide, in which there is a contact between the victim and the aggressor that may facilitate their transference from one to each other and to the crime scene [1–8]. In fact, when the fibres found in the crime scene, and especially on the victim, are the same as those from the suspect, that evidence is usually a convincing proof about the physical contact between both.

The visual microscopic examination of textile fibres is recommended by forensic experts because it allows a rapid differentiation of the fibres based on their morphological characteristics. However, the discrimination of fibres based on their perceptible colour and other non-specific visual properties is not always possible. In those cases, spectroscopic techniques are also used [8–10]. In fact, the forensic identification and comparison of fibres usually imply their characterization through different spectroscopic techniques such as ultraviolet–visible (UV–Vis) [11–16], infrared (IR) [17–20] and Raman spectroscopy [21–26]. IR and Raman spectroscopy are particularly suitable for this purpose since they enable a highly specific characterization of samples through their spectral "fingerprint", based on the chemical vibrations that molecules undergo during IR and Raman analysis [1,8,9]. In addition, these vibrational spectroscopic techniques can be coupled to microscopy, which make them highly useful in forensics.

In addition, besides the fibre identification, the analysis of fibres and fabrics by these vibrational spectroscopic techniques may also reveal other crucial aspects like the detection of traces of illicit substances such as drugs, explosives, or gunshot residues within the fibres [27–34]. The understanding of the spectral behaviour of fibres and fabrics is mandatory to exploit the capabilities of either IR or Raman spectroscopy for the fibres-comparison and the detection of exogenous substances within them.

Interestingly, some studies about the analysis of fibres by vibrational spectroscopic techniques have preliminary revealed a highly significant difference between IR and Raman spectroscopy regarding the fibres' spectral response. The IR spectrum of the fibre is mainly dominated by the spectral signature of the fibre-material, whereas the Raman spectrum results from the combination of the spectral signatures of both material and dyeing agents, with a larger predominance of the dyeing agents [9,11,23–26]. According to this, Raman spectroscopy is a bit more informative than IR, and what is more important, IR and Raman spectroscopy can be used complementarily to enhance the fibres discrimination. Nonetheless, further research in the textiles analysis by Raman spectroscopy is necessary to comprehend and make good use of the possibilities that Raman spectroscopy offers according to either the fibre composition or the dyes present in it.

Besides the traditional IR or Raman one-spot characterization of forensic evidence, chemical imaging modes are increasingly being used in forensics as a useful way to rapidly screen and provide the spectral chemical characterization of a large surface. Chemical imaging provides a result as clear and perceptible as a photograph of the evidence in which different compounds might be distinctively highlighted. This enables the visualization and easy discrimination of chemically different regions of the evidence, which may reveal the presence of different components that are interlaced, overlapped, or heterogeneously mixed [35–37]. Hence, this work examines, for the first time, the capabilities of Raman imaging [38] for the examination, discrimination and imaging of textile fibres and fabrics. Specifically, this study tested the suitability of Raman imaging and multivariate analysis through four different experiments regarding the discrimination of: (i) four white different cotton materials, (ii) blue cotton and blue polyester fabrics, (iii) five cotton fabrics of different colour, and (iv) five different fibres (acrylic, cotton, nylon, polyester and silk).

2. Experimental

2.1. Samples

A variety of textile samples made of 100 % cotton: gauze, cotton wool, swab, and white t-shirt, were studied as four white different materials. Cuts from six t-shirts of different colours (one of them made of 100 % polyester and five of them made of 100 % cotton) were selected to study cotton-polyester discrimination as well as the discrimination of the five cotton fabrics of different colour. These materials (cotton and polyester) are the two most relevant and predominant textile materials in clothing throughout the world [3,5]. Finally, five different textile fibres recovered on police adhesive tape were also studied. The fibres were sealed between two adhesive tape layers and directly analysed. The adhesive tape as well as the textile fibres (acrylic, cotton, nylon, polyester, and silk) were provided by *Guardia Civil* (Spanish Police Force). These textile fibres were part of the fibres collection gathered by the police forces over the years. Gauze, cotton wool, swab, and t-shirts were purchased from a Spanish local supermarket.

The cuts of gauze, cotton wool and t-shirts were less than 5x5 mm^2 size, with a thickness of 800 μm, approximately. The diameter of the textile fibres ranged from 10 to 25 μm, though fibres of some materials, particularly cotton, nylon and silk, were interlaced, making up strings whose diameters ranged between 300 and 600 μm.

2.2. Instrumentation for Raman imaging analysis

The Raman imaging measurements were performed on a Thermo DXRxi Raman imaging microscope (Thermo Fisher Scientific, Waltham, USA) equipped with an electron-multiplying charge-coupled device (EMCCD), a 455 nm excitation wavelength laser, and a 1200 lines mm^{-1} grating. The equipment was controlled using the OMNICxi Raman imaging software (1.0.0.2427; Thermo Fisher Scientific, Waltham, USA). The samples of the experiments 1, 2 and 4 were analysed setting 5 mW as laser power and 50 μm as the aperture slit size of the spectrograph. The samples of experiment 3 were analysed using 3 mW as laser power and with a 25 μm aperture slit size of the spectrograph. The laser power and spectrograph aperture were decreased in the experiment 3 in order to reduce the fluorescence of the dark fabrics, especially the black cotton fabric. In all the experiments, the measured spectral range covered from 3000 to 200 cm^{-1} Raman shift with a data spacing of around 1.93 cm^{-1}. Regarding the microscope objectives, the samples of the experiments 1, 2 and 3 (fabric cuts) were visualized using the 4x magnification objective whereas the samples of the experiment 4 (fibres) were visualized with the 10x magnification objective. Since the samples of the experiment 4 were fibres instead of fabric cuts, a larger magnification was necessary to visualize them properly.

The samples were analysed using the built-in line-scan mapping function, accumulating 200 scans per image, and using 0.06 s as exposure time for the fabrics and 0.02 s for the fibres. These high-speed exposures were performed thanks to the EMCCD detector which is very fast and amplified the signal through its electron multiplier register. This enabled reducing the acquisition time to 20–50 min per mapping (depending on the size of the sample). In addition, it should be remarked that the spectra were directly fluorescence-corrected during the collection. This is

because of the software option was set by default to avoid fluorescence, which involves the application of a polynomial of order six to correct the fluorescence. Thus, the raw spectra were directly obtained fluorescence-corrected.

It should be also noted that since each experiment recorded one Raman spectrum per pixel, the number of Raman spectra recorded for each sample depended on the number of pixels (2D size image). In this respect, it should be clarified that the image size varied in each experiment because of the sample's surface area and the focus enabled by the 4X or 10X magnification objective. In sum, around 100 Raman spectra were collected for each material in experiment 1 (*i.e.*, images of 10 × 10 pixels (100 pixels)); around 200 Raman spectra were collected for each fabric in experiment 2 (*i.e.*, images of 15 × 15 pixels (225 pixels)); around 50 Raman spectra were collected for each fabric in experiment 3 (*i.e.*, images of 7 × 7, or 8 × 6 pixels, (48–49 pixels)); and around 100 Raman spectra were collected for each fibre material in experiment 4 (*i.e.*, images of 10 × 10 pixels (100 pixels)).

2.3. Data treatment

The images obtained from the Raman imaging analysis were examined and processed following various procedures and treatments. First, all the spectra contained in the Raman images were unfolded using the Raman imaging software. Afterwards, the Raman spectra were imported as a matrix form into the The Unscrambler X 10.6 (Camo, Oslo, Norway) software. The spectra were smoothed and normalized in order to reduce the noise and the spectral intensity differences due to the mapping process so as to facilitate, thereby, the comparison among the spectra. The smoothing was performed by using the Savitzky-Golay algorithm considering a 2nd order polynomial along 15 smoothing points in a symmetric kernel. The normalization involved a range normalization.

The final multivariate analysis stage included principal component analysis (PCA) using The Unscrambler, multivariate analysis of variance (MANOVA) using Statgraphics Centurion XVII (Statgraphics Technologies, Virginia, USA), and colour chemical maps through multivariate curve resolution (MCR) using OMNICxi. The PCA was performed on mean centred data using 1/StdDev weights, and was validated using a random with 10 segments cross validation method. In summary, PCA was initially used in the four studies to explore and statistically visualize the data. MANOVA was used in the two first studies to mathematically ensure the alleged discrimination provided by PCA. The false colour chemical maps were studied in the two last studies, in which the different unknown samples were placed together in a single evidence and, thus, they were analysed in the same Raman image.

3. Results and discussion

3.1. Study of different cotton materials (t-shirt, swab, sterile gauze, and cotton wool)

The comparison among the Raman spectra from the different 100 % cotton materials (white T-shirt, swab, cotton wool, and gauze) was aimed to check the spectral variability among them despite that all are made of cotton. First of all, the Raman spectra collected within the mapping of each sample were averaged and visually compared (Fig. 1). In addition, Fig. S1 (in the supplementary material) shows the standard deviation obtained for each material when calculating the average Raman spectra, which is useful to visually estimate the spectral variability within each material.

According to Fig. 1, the four cotton materials showed almost identical and indistinguishable spectra due to the characteristic Raman signals coming from the cellulose (main component of cotton), except the t-shirt fibres, whose spectrum displayed an additional characteristic prominent band at 1600 cm^{-1}. This band clearly differentiated the t-shirt fibres from the other materials only characterized by the cellulose bands, which are located at 2896 cm^{-1} (C-H stretching), 1475 and 1380 cm^{-1} (CH_2 scissoring and C—H bending), 1335 cm^{-1} (O—H bending), and 1122 and 1094 cm^{-1} (C—O—C asymmetric and C—O—C symmetric stretching). The assignment of Raman bands to chemical vibrations, which is summarized in the supplementary Table S1, was assisted by revising the published literature about the Raman analysis of textile fibres [39–43]. The additional band at 1600 cm^{-1} in the t-shirt fibres spectra seems to indicate that there is not only cotton in its composition, but also another component. Since the t-shirt fibres were white, one could assume that no coloured dyes would be expected on the t-shirt's material. However, commercial fabrics are likely to contain some kind of bleaching agents or even some whiting dyes, which could explain this band at 1600 cm^{-1}. In fact, this spectral range is chemically related to aromatic C=C bonds, which are usually contained in organic dyes.

These spectra comparison was subsequently tackled using chemometrics. Particularly, a PCA was performed in order to explore the samples, reduce the variables, and statistically visualize the distribution of all spectra (which, are multitude of continuous data) from the four materials according to their spectral differences. Fig. 2 shows the scores PCA as well as the loadings plots.

The PCA statistically corroborated that t-shirt fibres are noticeably different from the fibres of the other three cotton-made materials since their scores were easily differentiated taking PC1 into consideration. As can be seen in the loading plots, PC1 was mainly affected by the band at 1600 cm^{-1}. Regarding the other three cotton-containing materials (gauze, swab and cotton wool fibres), they were closely distributed which would indicate that they have similar spectra. Even so and unexpectedly, PCA evidenced some differences for the swab fibres in comparison to the gauze and cotton wool fibres because their scores were located at a bit distance considering both PC1 and PC2. However, gauze and cotton wool still remained indistinguishable because their respective scores were intermingled conforming a single cluster. This result was more evident when a new PCA (Fig. S2) was recalculated only for gauze, cotton wool and swab (*i.e.,* after removing the Raman spectra from the T-shirt). As expected, the loadings of the new PCA were not influenced by the band at 1600 cm^{-1} that was exclusive for the T-shirt. On the contrary, the loading plots of the new PCA were the result of multiple slight spectral differences throughout the whole spectrum. Particularly, most swab scores were distributed along the positive values of PC1 (values > 1), and most gauze and cotton wool scores were distributed along the negative values of PC1. Gauze and cotton wool still remained undistinguishable in this PCA (Fig. S2).

The PCA results were subsequently confirmed using a MANOVA test based on PC1 and PC2 as the new reduced variables. Table 1 summarizes both the respective value and the existing variance within each cotton material for PC1 and PC2 (from the PCA displayed in Fig. 2). Regarding the discrimination, MANOVA confirmed that the swab and t-shirt samples had significant differences in relation to the other materials, therefore it was possible to statistically differentiate both swab and t-shirt fibres. On the other hand, the gauze and cotton wool samples were again indistinguishable. This fact was also checked from the values of both the gauze and cotton wool fibres for PC1 and PC2. They matched each other almost exactly and both were included within the same range when considering their variance.

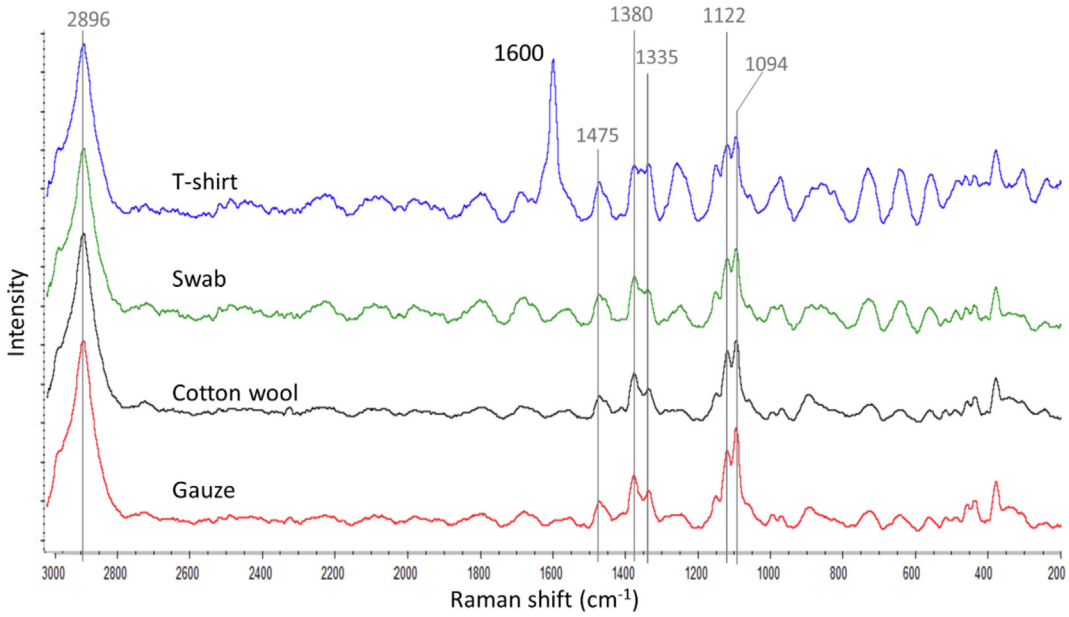

Fig. 1. Average Raman spectra from the white T-shirt (blue), swab (green), cotton wool (black), and gauze (red). All these samples were made of 100 % cotton.

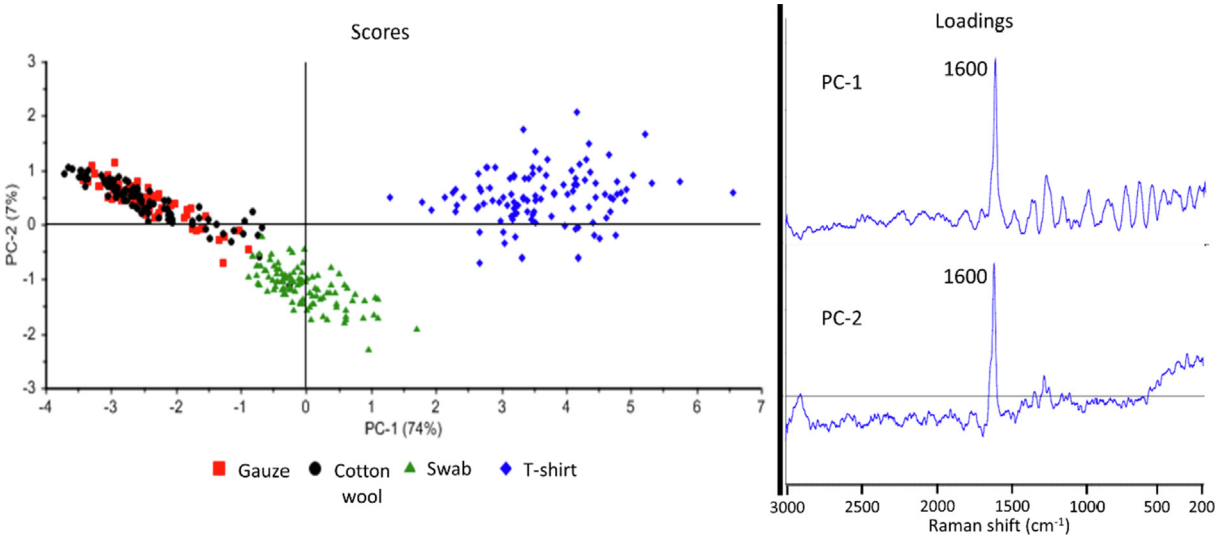

Fig. 2. Two-dimensional scores PCA plot of the Raman spectra from the four cotton materials (left): gauze (red square), cotton wool (black circle), swab (green triangle), and t-shirt (blue diamond). The PCA model is explained by PC1 (74 %) and PC2 (7 %). Line loadings plot from PC1 and PC2 (right).

Table 1
MANOVA results from the four different cotton materials (t-shirt, swab, gauze, and cotton wool).

Materials	PC1	PC2
Gauze	−2.45 ± 0.6	0.43 ± 0.4
Cotton wool	−2.44 ± 0.7	0.42 ± 0.4
Swab	−0.03 ± 0.5	−1.15 ± 0.3
T-shirt	3.64 ± 0.9	0.51 ± 0.5

3.2. Study of the different materials (cotton and polyester) with the same perceptible colour (blue)

In order to check whether Raman imaging enables the discrimination of fabrics of the same colour but made of different materials, this work studied blue fabrics made of either 100 % cotton or 100 % polyester. It is widely known that UV–Vis hyperspectral imaging has some deficiencies regarding the discrimination of fabrics since the visible radiation is mainly determined by the colour of the fabric rather than its composition. On the contrary, Raman dispersion provides a chemical characterization of the evidence because of the Raman active chemical bonds contained in the sample. As displayed in Fig. 3, both blue fabrics (cotton and polyester) were easily differentiated according to their average Raman spectra even to the naked eye. Fig. S3 (supplementary material) shows the standard deviation obtained within each material. The blue cotton fabric was dominated by three intense bands located at 1582, 1409 and 1270 cm^{-1}; whereas the blue polyester fabric showed five characteristic bands at 1725, 1614, 1292, 856, and 633 cm^{-1}. It should be noted that these spectral differences are

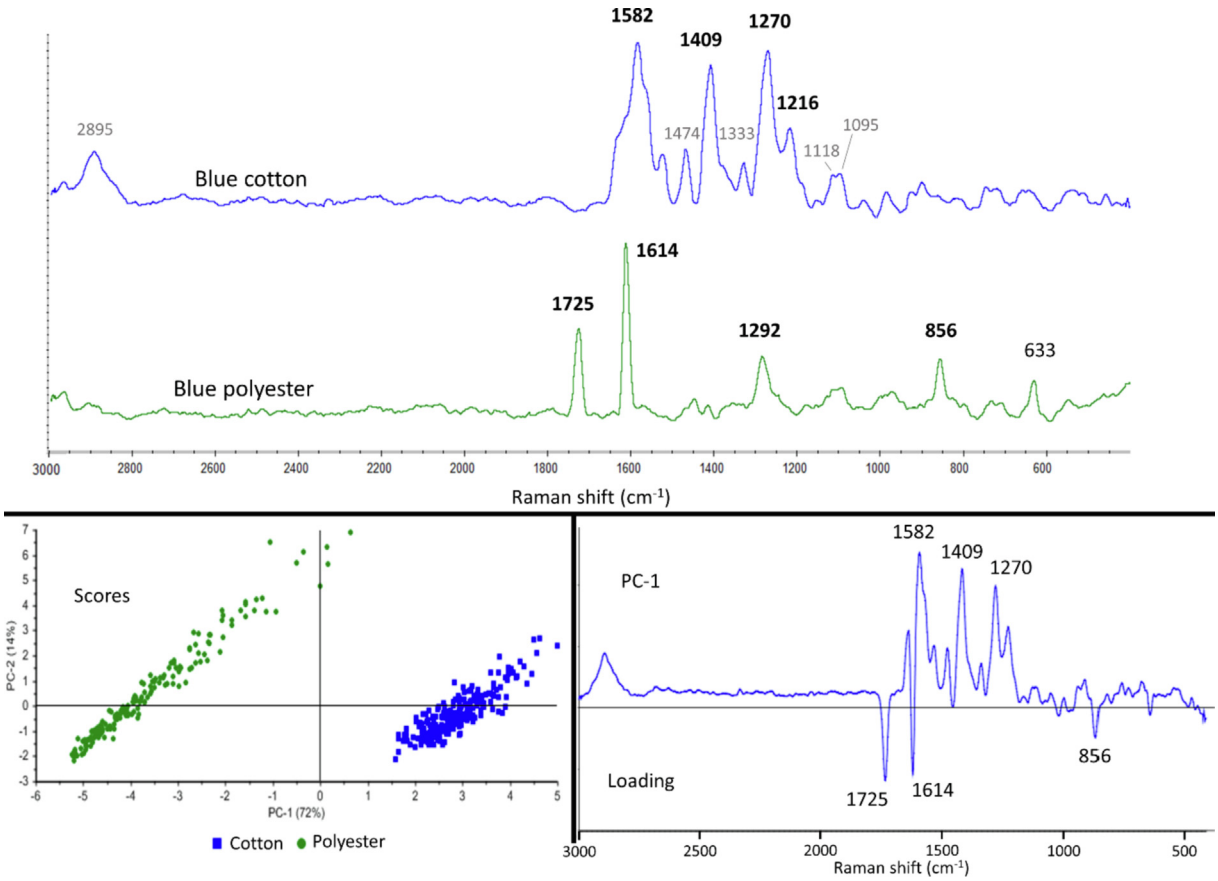

Fig. 3. Average Raman spectra from the blue cotton T-shirt (blue) and blue polyester T-shirt (green) samples (above). Two-dimensional scores PCA plot of the Raman spectra from the two blue T-shirts: cotton (blue squares) and polyester (green circles) (bottom left). The PCA model was explained by the PC1 (72 %) and PC2 (14 %). Line loadings plot from PC1 (bottom right).

likely due to two factors: i) the different material (cotton or polyester), and ii) the different blue dyeing agent. In this case, the dying agent is unknown because the dyes composition is not provided by the manufacturers. However, it is known that even though both blue materials look visually of the same blue colour, different blue dyes have necessarily been used. This is because different textile materials are dyed by different methods and by chemically different dyeing agents (those which are optimum for that material). In fact, polyester fibres are normally dyed using disperse dyes, whereas cotton fibres are normally dyed using reactive, direct or vat dyes. Thus, in this case, the Raman spectral differences are likely due to both the different material and the different dyeing agent. As summarized in Table S1, in the blue cotton spectrum the bands at 2895, 1474, 1333, 1118, and 1095 cm^{-1} due to cotton are lesser intense than the bands at 1582, 1409, and 1270 cm^{-1} coming from the blue dying agent. On the contrary, the blue polyester spectrum was dominated by the bands at 1725, 1614, 1292 and 856 cm^{-1} which are respectively due to C=O (ester) stretching, C=C aromatic stretching, O—C—O stretching, and C—H bending of polyethylene terephthalate (PET), which is the main component of polyester textile fibres [39,40,44]. According to this result, the polyester material is more Raman active than the cotton material.

Though already differentiated by visually comparing their different Raman spectra, further studies using PCA (also displayed in Fig. 3) and the F-test corroborated the clear discrimination of both fabrics. Regarding the PCA, PC1 successfully explained the differentiation of both fabrics (cotton and polyester) since they were located separately. The cotton was located towards the PC1 positive values, explained by the bands at 1582, 1409, and 1270 cm^{-1}, whilst polyester was located towards the PC1 negative values (bands at 1725, 1614, and 856 cm^{-1}). Taking advantage of the well-defined PCA plot containing only two clusters, the MANOVA, or in this case the F test, was easily calculated this time by means of the Mahalanobis distance (25.6) and T^2 Hotelling value (65634). Since the F calculated was larger than the F tabulated (32736 > 3), the null hypothesis was rejected, which means that the two fabrics were found different and distinguishable.

3.3. Study of the 100 % cotton fabrics of different colour (green, blue, red, black, and white)

After easily discriminating fabrics of different composition (shown in the previous experiment), the suitability of Raman imaging to discriminate fabrics made of the same material (*i.e.,* 100 % cotton), but different colours, was evaluated. Thus, Raman imaging was tested for discriminating coloured cotton fabrics *i.e.*, exclusively according to the dyes that provide the characteristic colour to cotton clothes. Positively, the results showed significant spectral differences among the various coloured T-shirts made of 100 % cotton, particularly within the 1000–1700 cm^{-1} range (Fig. 4). The standard deviation obtained within each coloured cotton fabrics is also displayed in the right side of Fig. 4.

In brief, the Raman spectra of cotton fabrics were dominated by the dying agent characteristic bands. The exception was the white cotton fabric whose Raman bands come from the cotton material (cellulose) apart from the band at 1600 cm^{-1} previously observed in experiment 1, which is due to some whiting dye. On the contrary, the most intense bands of green cotton fabric were located

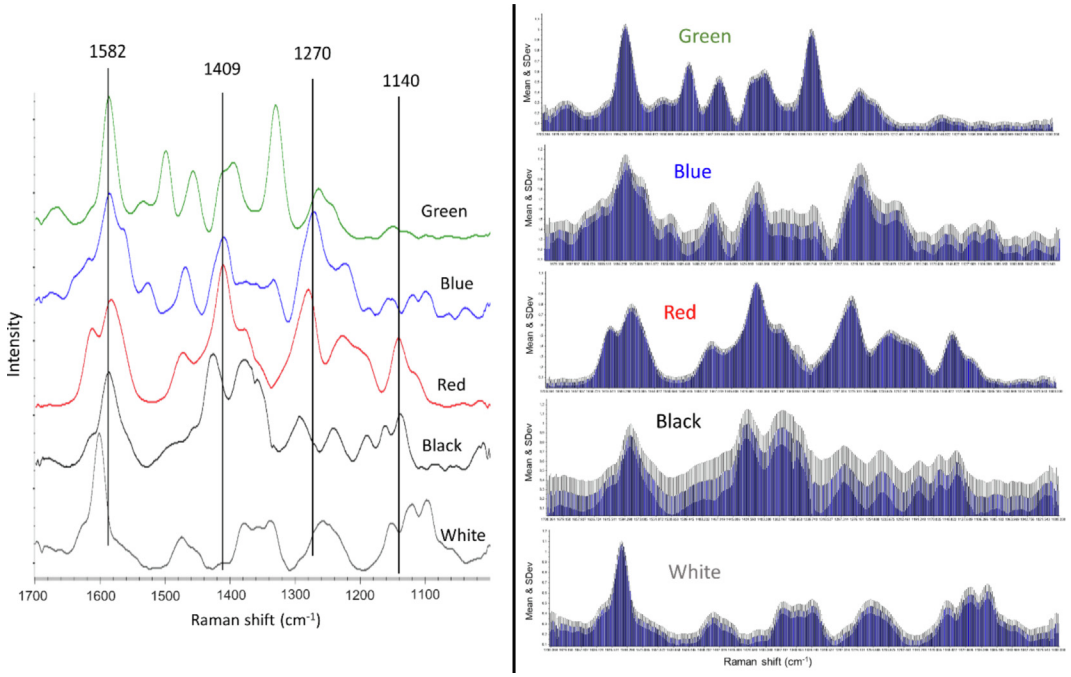

Fig. 4. (Left) Average Raman spectra from the five T-shirts made of 100 % cotton dyed as follows: green (green), blue (blue), red (red), black (black), and white (grey); (Right) Standard deviation of the Raman spectrum within each fabric.

at 1583, 1500, 1456, 1409, and 1395 cm^{-1}. They were not the characteristic bands of cellulose (cotton material); thus, they must come from the green dyeing agent. As summarized in supplementary Table S1, the same occurred for: i) the blue cotton fabric whose most intense bands (1582, 1409, 1270, and 1219 cm^{-1}) were due to the blue dyeing agent; ii) the red cotton fabric whose most intense bands (1614, 1581, 1411, 1278, 1227, and 1141 cm^{-1}) were due to the red dyeing agent; and iii) the black cotton fabric whose bands (1426, 1378, 1359, 1292, 1241, 1189, 1162, and 1141 cm^{-1}) were all due to the black dyeing agent.

The Raman discrimination of fabrics was confirmed by PCA (Fig. 5). This method was able to separate all the t-shirts by their colour. In other words, the Raman spectra from each coloured T-shirt were placed near each other but separated from the other T-shirts. Interestingly, the Raman spectra from red, green and white T-shirts gave less dispersion (*i.e.*, less deviation) than either the blue or the black ones whose scores were more dispersed along the PCA plot, which is also in accordance with Fig. 4. This could be explained by the fact that these darker colours usually display more fluorescence when analysed by Raman spectroscopy than lighter coloured materials. Even though the fluorescence correction instrumental option was applied, it is checked that is not infallible; and high fluorescent colours usually provides larger Raman spectral deviations.

The available colour chemical mapping option of the Raman software was tested on the coloured fabrics (blue, red, green, and black), all made of cotton. They were set together in the same view field, and so the spectra were collected within the same image in such a way that a region of each fabric was captured and analysed simultaneously (Fig. 6). This colour chemical mapping involved the selection of an averaged Raman spectrum which was subsequently compared against the Raman spectra from all the pixels located within the registered regions of the image. Such comparison or matching was performed using multivariate curve resolution (MCR). In brief, MCR is a statistical correlation procedure that searches the selected spectrum all throughout the image. As an example, Fig. 6 shows the chemical maps obtained after selecting an averaged Raman spectrum of the red cotton fabric. This spectrum would be the one to be "searched" and statistically matched against all the other spectra along the entire image. The four registered squared regions are coloured according to the spectral similarities of their pixels-spectra with the selected Raman spectrum displayed in the bottom of the image. As expected, the regions of either the blue, green or black cotton fabrics displayed blue to green false coloured maps which implies a low correlation with the selected spectrum. On the contrary, the region of the red cotton fabric is almost completely red in the false colour map, which implies a high correlation between those spectra and the test spectrum.

3.4. Study of five different fibres recovered on adhesive tape: Approaching forensic caseworks

The last stage was to examine the capability and response of Raman imaging when dealing with typical fibres found as evidence from forensic caseworks. Hence, this step analysed five different randomly selected types of fibres (dark-blue acrylic, dark-blue polyester, brownish nylon, black silk, and brown cotton) recovered using the police adhesive tape. Fig. 7 shows the average Raman spectra from the five fibres. In addition, Fig. S4 (supplementary material) shows the standard deviation obtained within each fibre. The main result involved the detection of all the fibres by Raman imaging (using the 10x magnification). In other words, the five fibres' characteristic Raman signals were detected over the signal of the adhesive tape. This is a great advantage in forensics because the fibres evidence (sealed between two adhesive tape layers) was directly screened and identified using Raman imaging without unsealing the evidence. In addition, the five fibres were distinguishable according to their different Raman spectra even to the unaided eye. As previously indicated, it should be noted that the characteristic Raman spectrum of each fibre was due to both the raw material and the dyeing agent giving the colour to the fibre.

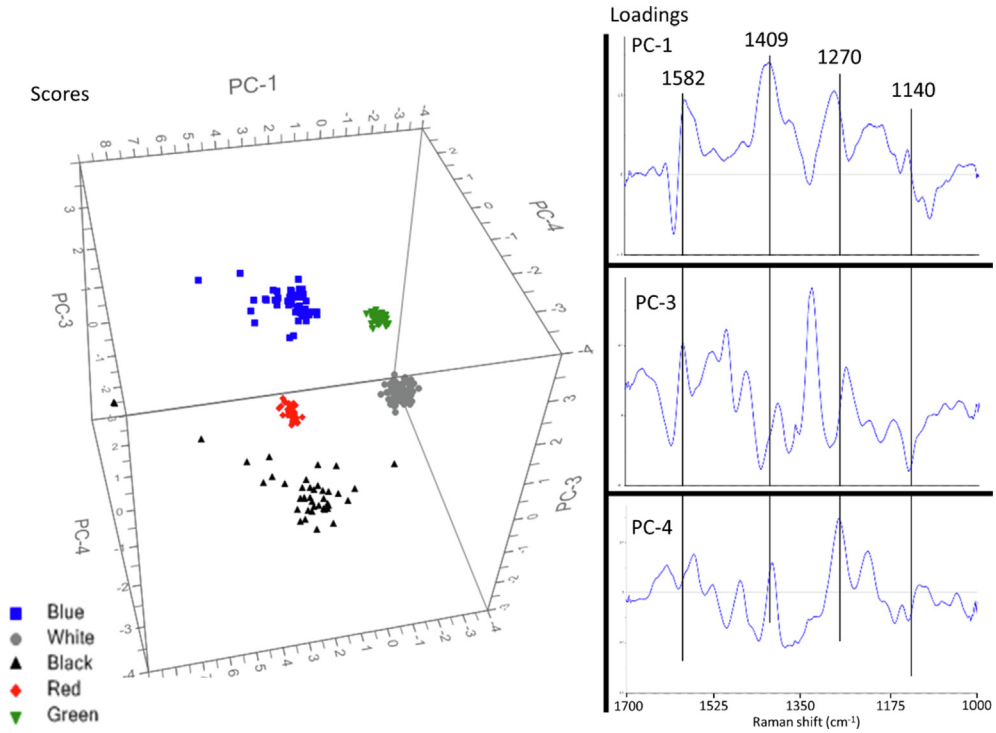

Fig. 5. Three-dimensional scores PCA plot of the Raman spectra from the five coloured cotton T-shirts (left): blue (blue square), white (grey circle), black (black triangle), red (red diamond), and green (green inverted triangle). The PCA model was explained by the PC1 (39 %), PC3 (15 %), and PC4 (12 %). Line loadings plot from PC1, PC3 and PC4 (right).

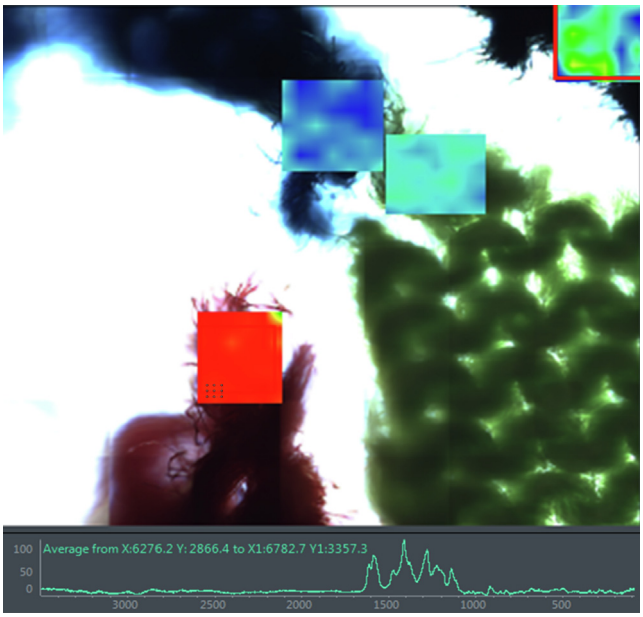

Fig. 6. False colour chemical map tested on the coloured fabrics (blue, red, green, and black), all made of cotton. The dot matrix represents a sampling point-array in the fabric for reading several spectra and creating an averaged Raman spectrum (bottom) of the red cotton T-shirt.

In this case, most fibres also displayed the characteristic bands of the adhesive tape in the 3000–2800 cm^{-1} region, which is due to C-H stretching. As summarized in supplementary Table S1, dark-blue acrylic fibre displayed the characteristic bands of both the acrylic material (mainly polyacrylonitrile, PAN) and the blue dyeing agent. The PAN bands were located at 2242 cm^{-1} (nitrile C≡N stretching), and 1470 and 1332 cm^{-1} (CH_2, CH bending) [39,40], whereas the additional bands (1606, 1561, 1243, and 1129 cm^{-1}) were likely due to the blue dye. The dark-blue polyester fibre also displayed bands from the polyester (PET) material (1727, 1613, and 1286 cm^{-1}) [39,40,44], and from the dyeing agent (1575, 1450, and 1345 cm^{-1}). The low intense bands (2911, 1447, and 1130 cm^{-1}) observed in the Raman spectrum of the brownish nylon fibre were mostly due to the nylon (polyamide (PA)) material [39,40], and from the adhesive tape (2940, and 2880 cm^{-1}). On the contrary, the low intense bands (1596, and 1565 cm^{-1}) observed in the Raman spectrum of the black silk fibre were likely due to the black dyeing agent. The exception would be the band at 1253 cm^{-1}, which is characteristic of the silk material (Amide III vibration) [39,40], and the bands at 2940 and 2882 cm^{-1} due to the adhesive tape. Finally, the brown cotton fibre displayed bands from both the cotton material (1473, 1334, and 1126 cm^{-1}) [39–43], the brown dye (1600 and 1242 cm^{-1}), and the adhesive tape (2940 and 2880 cm^{-1}).

Unlike the previous experiments in which the cotton/polyester materials were new and were analysed just after being purchased; the police-donated fibres analysed in this last experiment were not new but collected by the police over several years. Hence, those fibres might be contaminated with dust (before being collected by police), and/or they might have been exposed to light and time aging. Unfortunately, the information about such factors is unknown for those fibres (as normally occur in real forensic practice). However, these factors are known to partially influence the Raman spectra of textile fibres. Thus, in this case, the Raman spectra of fibres, which is mainly due to the material and the dyeing agent, might be also slightly influenced by these uncontrolled factors. In extreme situations, which is not the case, these limiting factors might affect the characteristic Raman spectrum of the fibres, thus making more difficult the comparison of two potentially matching fibres.

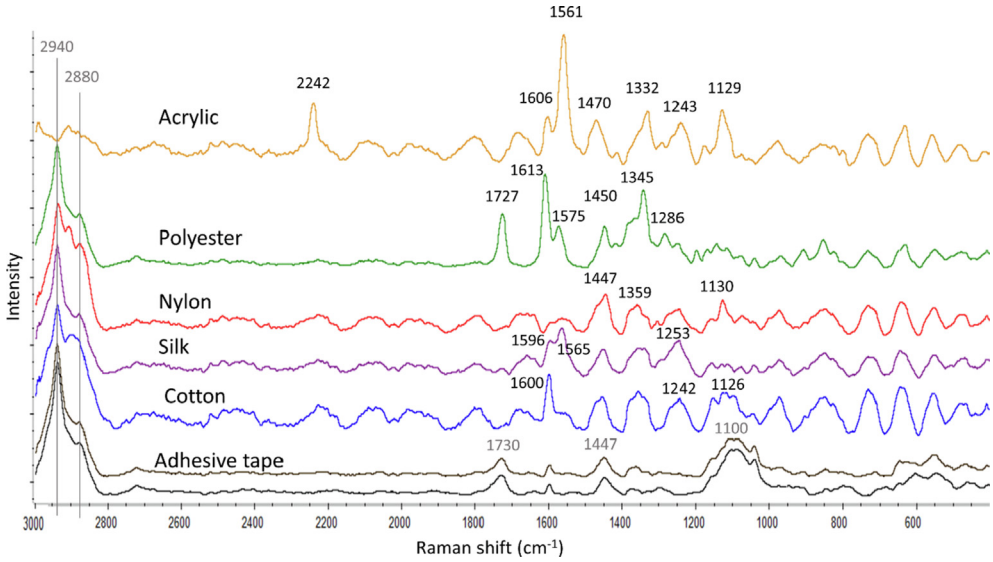

Fig. 7. Average Raman spectra from the five different fibres: dark-blue acrylic, dark-blue polyester, brownish nylon, black silk, and brown cotton; and average Raman spectra from the adhesive tape (the brown one from the adhesive side and the black one from the non-adhesive side).

In the studied fibres, those uncontrolled factors did not affect the fibres identification because the subsequent PCA analysis statistically corroborated the discrimination of the fibres (Fig. 8). In general, the five fibres' scores were located separately one to each other, being cotton and nylon the two more closely distributed with some intermediate spots that could be confused. In this case, the dispersion within each group was similar.

In order to study a more challenging evidence, it was decided to test the Raman imaging and the MCR colour mapping on a crossing fibre problem. Fig. 9 shows the mixed (crossing fibre) evidence analysed by Raman imaging and the corresponding results obtained using the colour chemical mapping.

From these two analysed crossing scenarios, one of them included white nylon fibres crossing blue polyester fibres, while the other one included white cotton fibres crossing black silk fibres (all sealed between two adhesive tape layers). As an example, an average Raman spectrum from the polyester fibres (first scenario) or the cotton fibres (second scenario) was selected to perform their corresponding colour chemical mapping. As previously explained, the red regions in the chemical image correspond to those pixels containing a Raman spectrum MCR-statistically similar to a selected spectrum, whereas the blue and green colours correspond to those pixels containing a statistically different spectrum. Noticeably, the respective fibres were partially red coloured whereas the opposite fibres appeared quite well defined in green colour.

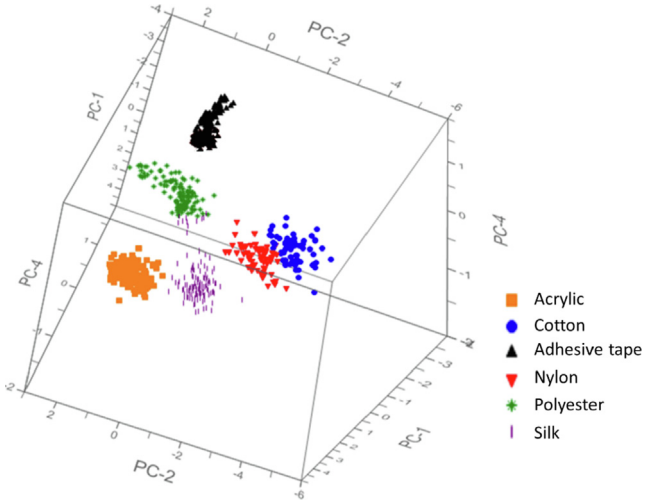

Fig. 8. Three-dimensional scores PCA plot of the Raman spectra from the five fibres and adhesive tape: acrylic (orange square), cotton (blue circle), adhesive tape (black triangle), nylon (red inverted triangle), polyester (green cross), and silk (purple vertical line). The PCA model is explained by the PC1 (48 %), PC2 (22 %), and PC4 (4 %).

4. Conclusions and future trends

In this work, Raman micro-spectroscopy showed enough selectivity to discriminate fabrics and fibres. In fact, it was verified how the Raman spectrum was determined by both the fabric's material and the colour (dyeing agents) present within the fibres. Thus, the chemical bonds from the material composition and the dyeing substances are both responsible for the Raman spectra of the fibres, depending on which one is more Raman active. As an example, slight but significant spectral differences were found among the white different materials made of 100 % cotton (gauze, cotton wool, swab, and t-shirt), and among the five 100 % cotton T-shirts of different colour. This implies additional chemical differences besides those given by the manufacturer about the material composition.

Since the Raman spectrum of a fibre is influenced by both the material and the dyeing agents, the potential and suitability of Raman imaging to discriminate fibres evidence is very high. This is especially important considering the large number of textile manufacturers and the wide variability in the clothing (including the dyeing agents) that people (aggressor, victim, witnesses, etc.) may wear. Particularly in this study, Raman imaging enabled the chemical visualization of the sealed fibres evidence using Raman chemical maps in which the distribution of the desired component along the pixels of the image is indicated in red intense colour. Thus, the use of a Raman imaging micro-spectrometer may extraordinarily support the microscopic examination of fibres. This procedure would increase the fibres analysis only for a few minutes during the Raman spectra collection since the MCR chemical

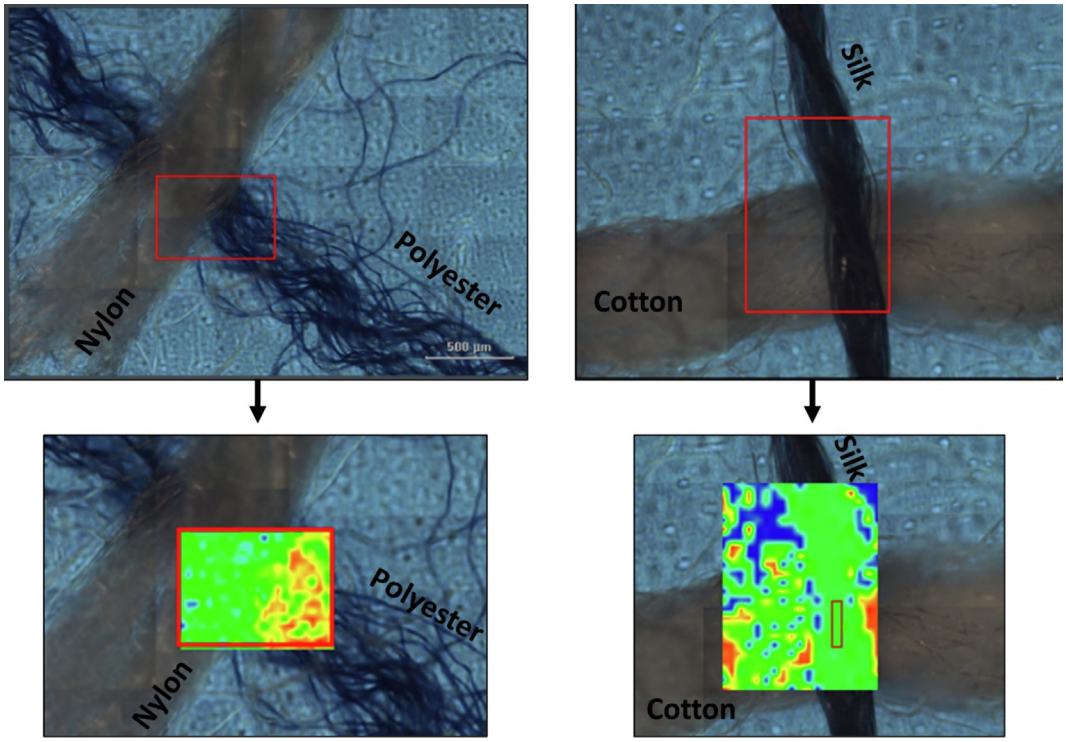

Fig. 9. Some crossing fibre evidence (sealed between two adhesive tape layers): white nylon fibres crossing blue polyester fibres (left), and white cotton fibres crossing black silk fibres (right). Colour chemical maps of each crossing fibre case after selecting an averaged Raman spectrum of polyester and cotton, respectively (bottom).

imaging is almost instantaneous in such instrumentation. It should be noted that even though the fibres and fabrics collected and analysed in this study represent a small sample, and even though the material is known, but the dyeing agents are unknown; the results from this study are representative to the pursued aim. This is because from a forensic point of view, not knowing the dyes is not a problem because comparative analyses between doubted-undoubted samples are frequently made. If their spectra are statistically similar, it is probable evidence of potential matching fabrics (both from the same manufacturer). If their spectra are clearly different, it is certain evidence of different fabric materials. Particularly, in case of extreme external factors (light, aging in external conditions, dust, etc.) the deterioration of the material could be simulated in the undoubted sample to compare them and see if there is any similarity. However, this is a topic that requires future research.

Finally, it should be noted that even though the aim of this study was the forensic examination of fibres, this methodology would be also useful to the analysis of textile fibres and clothing fabrics for other purposes such as quality control in textile manufacture.

CRediT authorship contribution statement

Félix Zapata: Conceptualization, Investigation, Writing – original draft, Writing – review & editing. **Fernando E. Ortega-Ojeda:** Investigation, Writing – review & editing. **Carmen García-Ruiz:** Conceptualization, Investigation, Writing – review & editing.

Declaration of Competing Interest

The authors declare that they have no known competing financial interests or personal relationships that could have appeared to influence the work reported in this paper.

Acknowledgements

The authors thank *Thermo Fisher Scientific Inc.* for kindly providing us access to the DXRxi Raman Imaging microscope for performing the experiments. The authors also thank *Guardia Civil* for kindly providing the adhesive tape and textile fibres studied in this work.

Appendix A. Supplementary material

Supplementary data to this article can be found online at https://doi.org/10.1016/j.saa.2021.120695.

References

[1] E.G. Bartick, Applications of Vibrational Spectroscopy in Criminal Forensic Analysis, in: J.M. Chalmers, P.R. Griffiths (Eds.), Handbook of Vibrational Spectroscopy, John Wiley & Sons, Chichester, 2002.
[2] M.M. Houck (Ed.), Identification of textile fibers, Woodhead Publishing Limited, 2009.
[3] M.C. Grieve, A survey on the evidential value of fibres and on the interpretation of the findings in fibre transfer cases. Part 1 - fibre frequencies, Sci. Justice 40 (3) (2000) 189–200, https://doi.org/10.1016/S1355-0306(00)71975-7.
[4] M.C. Grieve, T.W. Biermann, K. Schaub, The individuality of fibres used to provide forensic evidence - not all blue polyesters are the same, Sci. Justice 45 (1) (2005) 13–28, https://doi.org/10.1016/S1355-0306(05)71616-6.
[5] T.W. Biermann, Blocks of colour IV: The evidential value of blue and red cotton fibres, Sci. Justice 47 (2) (2007) 68–87, https://doi.org/10.1016/j.scijus.2006.08.001.
[6] S. Suzuki, Y. Higashikawa, R. Sugita, Y. Suzuki, Guilty by his fibers: suspect confession versus textile fibers reconstructed simulation, Forensic Sci. Int. 189 (1-3) (2009) e27–e32, https://doi.org/10.1016/j.forsciint.2009.03.035.
[7] J.V. Goodpaster, E.A. Liszewski, Forensic analysis of dyed textile fibers, Anal. Bioanal. Chem. 394 (8) (2009) 2009–2018, https://doi.org/10.1007/s00216-009-2885-7.
[8] P. Prego-Meleiro, C. García-Ruiz, Spectroscopic techniques for the forensic analysis of textile fibers, Appl. Spectrosc. Rev. 51 (4) (2016) 278–301, https://doi.org/10.1080/05704928.2015.1132720.
[9] L. Lepot, K. De Wael, F. Gason, B. Gilbert, Application of Raman spectroscopy to forensic fibre cases, Sci. Justice 48 (3) (2008) 109–117, https://doi.org/10.1016/j.scijus.2007.09.013.

[10] P. Buzzini, G. Massonnet, The analysis of colored acrylic, cotton, and wool textile fibers using micro-Raman spectroscopy. Part 2: Comparison with the traditional methods of fiber examination, J. Forensic Sci. 60 (3) (2015) 712–720, https://doi.org/10.1111/1556-4029.12654.
[11] S. Suzuki, Y. Suzuki, H. Ohta, R. Sugita, Y. Marumo, Microspectrophotometric discrimination of single fibres dyed by indigo and its derivatives using ultraviolet-visible transmittance spectra, Sci. Justice 41 (2) (2001) 107–111, https://doi.org/10.1016/S1355-0306(01)71861-8.
[12] S. L. Morgan, A. A. Nieuwland, C. R. Mubarak, J. E. Hendrix, E. M. Enlow, B. J. Vasser, Forensic Discrimination of Dyed Textile Fibers using UV-VIS and Fluorescence Microspectrophotometry, in: Proceedings of the European Fibres Group (Annual Meeting, Prague, Czechoslovakia, 25 May 2004).
[13] R. Palmer, W. Hutchinson, V. Fryer, The discrimination of (non-denim) blue cotton, Sci. Justice 49 (1) (2009) 12–18, https://doi.org/10.1016/j.scijus.2008.07.001.
[14] M. Eng, P. Martin, C. Bhagwandin, The analysis of metameric blue fibers and their forensic significance, J. Forensic Sci. 54 (4) (2009) 841–845, https://doi.org/10.1111/j.1556-4029.2009.01079.x.
[15] C. Wang, Q. Chen, M. Hussain, S. Wu, J. Chen, Z. Tang, Application of principal component analysis to classify textile fibers based on UV-Vis diffuse reflectance spectroscopy, J. Appl. Spectrosc. 84 (3) (2017) 391–395, https://doi.org/10.1007/s10812-017-0481-8.
[16] V. Sharma, R. Kumar, P. Kaur, Forensic examination of textile fibers using UV-VIS spectroscopy combined with multivariate analysis, J. Appl. Spectrosc. 86 (1) (2019) 96–100, https://doi.org/10.1007/s10812-019-00787-4.
[17] S. Cantrell, C. Roux, P. Maynard, J. Robertson, A textile fibre survey as an aid to the interpretation of fibre evidence in the Sydney region, Forensic Sci. Int. 123 (1) (2001) 48–53, https://doi.org/10.1016/S0379-0738(01)00520-5.
[18] K. Wiggins, P. Drummond, T. Hicks Champod, A study in relation to the random distribution of four fibre types on clothing (incorporating a review of previous target fibre studies), Sci. Justice 44 (3) (2004) 141–148, https://doi.org/10.1016/S1355-0306(04)71706-2.
[19] V. Causin, C. Marega, S. Schiavone, A. Marigo, A quantitative differentiation method for acrylic fibers by infrared spectroscopy, Forensic Sci. Int. 151 (2-3) (2005) 125–131, https://doi.org/10.1016/j.forsciint.2005.02.004.
[20] T. Sano, S. Suzuki, Basic forensic identification of artificial leather for hit-and-run cases, Forensic Sci. Int. 192 (1-3) (2009) e27–e32, https://doi.org/10.1016/j.forsciint.2009.08.018.
[21] J.V. Miller, E.G. Bartick, Forensic Analysis of Single Fibers by Raman Spectroscopy, Appl. Spectrosc. 55 (12) (2001) 1729–1732, https://doi.org/10.1366/0003702011954099.
[22] J. Thomas, P. Buzzini, G. Massonnet, B. Reedy, C. Roux, Raman spectroscopy and the forensic analysis of black/grey and blue cotton fibres. Part 1. Investigation of the effects of varying laser wavelength, Forensic Sci. Int. 152 (2-3) (2005) 189–197, https://doi.org/10.1016/j.forsciint.2004.08.009.
[23] G. Massonnet, P. Buzzini, G. Jochem, M. Stauber, T. Coyle, C. Roux, J. Thomas, H. Leijenhorst, Z. Van Zanten, K. Wiggins, C. Russell, S. Chabli, A. Rosengarten, Evaluation of Raman Spectroscopy for the Analysis of Colored Fibers: A Collaborative Study, J. Forensic Sci. 50 (5) (2005) 1–11, https://doi.org/10.1520/JFS2004532.
[24] G. Jochem, R.J. Lehnert, On the potential of Raman microscopy for the forensic analysis of coloured textile fibres, Sci. Justice 42 (4) (2002) 215–221, https://doi.org/10.1016/S1355-0306(02)71831-5.
[25] G. Massonnet, P. Buzzini, F. Monard, G. Jochem, L. Fido, S. Bell, M. Stauber, T. Coyle, C. Roux, J. Hemmings, H. Leijenhorst, Z. Van Zanten, K. Wiggins, C. Smith, S. Chabli, T. Sauneuf, A. Rosengarten, C. Meile, S. Ketterer, A. Blumer, Raman spectroscopy and microspectrophotometry of reactive dyes on cotton fibres: Analysis and detection limits, Forensic Sci. Int. 222 (1-3) (2012) 200–207, https://doi.org/10.1016/j.forsciint.2012.05.025.
[26] P. Buzzini, G. Massonnet, The discrimination of colored acrylic, cotton, and wool textile fibers using micro-Raman spectroscopy. Part 1: In situ detection and characterization of dyes, J. Forensic Sci. 58 (6) (2013) 1593–1600, https://doi.org/10.1111/1556-4029.12298.
[27] E.M.A. Ali, H.G.M. Edwards, M.D. Hargreaves, I.J. Scowen, In-situ detection of drugs-of-abuse on clothing using confocal Raman microscopy, Anal. Chim. Acta 615 (1) (2008) 63–72, https://doi.org/10.1016/j.aca.2008.03.051.
[28] M.J. West, M.J. Went, The spectroscopic detection of drugs of abuse on textile fibres after recovery with adhesive lifters, Forensic Sci. Int. 189 (1-3) (2009) 100–103, https://doi.org/10.1016/j.forsciint.2009.04.024.
[29] E.M.A. Ali, H.G.M. Edwards, I.J. Scowen, Rapid in-situ detection of street samples of drugs of abuse on textile substrates using microRaman spectroscopy, Spectrochim. Acta A 80 (1) (2011) 2–7, https://doi.org/10.1016/j.saa.2010.11.001.
[30] E.M.A. Ali, H.G.M. Edwards, Screening of textiles for contraband drugs using portable Raman spectroscopy and chemometrics, J. Raman Spectrosc. 45 (3) (2014) 253–258, https://doi.org/10.1002/jrs.4444.
[31] L. Xiao, R. Alder, M. Mehta, N. Krayem, B. Cavasinni, S. Laracy, S. Cameron, S. Fu, Development of a quantitative method for the analysis of cocaine analogue impregnated into textiles by Raman spectroscopy, Drug Test. Anal. 10 (4) (2018) 761–767, https://doi.org/10.1002/dta.v10.410.1002/dta.2261.
[32] E.M.A. Ali, H.G.M. Edwards, I.J. Scowen, In-situ detection of single particles of explosive on clothing with confocal Raman microscopy, Talanta 78 (3) (2009) 1201–1203, https://doi.org/10.1016/j.talanta.2008.12.038.
[33] E.M.A. Ali, H.G.M. Edwards, I.J. Scowen, Raman spectroscopy and security applications: the detection of explosives and precursors on clothing, J. Raman Spectrosc. 40 (12) (2009) 2009–2014, https://doi.org/10.1002/jrs.2360.
[34] S. Charles, M. Lannoy, N. Geusens, Influence of the type of fabric on the collection efficiency of gunshot residues, Forensic Sci. Int. 228 (1-3) (2013) 42–46, https://doi.org/10.1016/j.forsciint.2013.02.022.
[35] K. Flynn, R. O'Leary, C. Roux, B.J. Reedy, Forensic Analysis of Bicomponent Fibers Using Infrared Chemical Imaging, J. Forensic Sci. 51 (3) (2006) 586–596, https://doi.org/10.1111/j.1556-4029.2006.00116.x.
[36] A.-Y. Lin, H.-M. Hsieh, L.-C. Tsai, A. Linacre, J.-I. Lee, Forensic applications of infrared imaging for the detection and recording of latent evidence, J. Forensic Sci. 52 (5) (2007) 1148–1150, https://doi.org/10.1111/j.1556-4029.2007.00502.x.
[37] G.J. Edelman, E. Gaston, T.G. van Leeuwen, P.J. Cullen, M.C.G. Aalders, Hyperspectral imaging for non-contact analysis of forensic traces, Forensic Sci. Int. 223 (1-3) (2012) 28–39, https://doi.org/10.1016/j.forsciint.2012.09.012.
[38] S. Stewart, R.J. Priore, M.P. Nelson, P.J. Treado, Raman Imaging, Annu. Rev. Anal. Chem. 5 (1) (2012) 337–360, https://doi.org/10.1146/annurev-anchem-062011-143152.
[39] L. Cho, Identification of textile fiber by Raman microspectroscopy, Forensic Sci. J. 6 (1) (2007) 55–62.
[40] D. Puchowicz, M. Cieslak, Raman spectroscopy in the analysis of textile structures, IntechOpen (2021), https://doi.org/10.5772/intechopen.99731.
[41] U.P. Agarwal, Analysis of cellulose and lignocellulose materials by Raman spectroscopy: A review of the current status, Molecules 24 (2019) 1659, https://doi.org/10.3390/molecules24091659.
[42] A. Rygula, K. Jekiel, J. Szostak-Kot, T.P. Wrobel, M. Baranska, Application of FT-Raman spectroscopy for in situ detection of microorganisms on the surface of textiles, J. Environ. Monit. 13 (11) (2011) 2983, https://doi.org/10.1039/c1em10698h.
[43] D. Puchowicz, P. Giesz, M. Kozanecki, M. Cieslak, Surface-enhanced Raman spectroscopy (SERS) in cotton fabric analysis, Talanta 195 (2019) 516–524, https://doi.org/10.1016/j.talanta.2018.11.059.
[44] E. Rebollar, S. Pérez, M. Hernández, C. Domingo, M. Martín, T.A. Ezquerra, J.P. García-Ruiz, M. Castillejo, Physicochemical modifications accompanying UV laser induced surface structures on poly(ethyleneterephthalate) and their effect on adhesion of mesenchymal cells, Phys. Chem. Chem. Phys. 16 (33) (2014) 17551, https://doi.org/10.1039/C4CP02434F.